HAL
open science

Emergence of coexistence and limit cycles in the chemostat model with flocculation for a general class of functional responses

Radhouane Fekih-Salem, Alain Rapaport, Tewfik Sari

To cite this version:

Radhouane Fekih-Salem, Alain Rapaport, Tewfik Sari. Emergence of coexistence and limit cycles in the chemostat model with flocculation for a general class of functional responses. 2015. hal-01121201

HAL Id: hal-01121201

https://inria.hal.science/hal-01121201v1

Preprint submitted on 27 Feb 2015

HAL is a multi-disciplinary open access archive for the deposit and dissemination of scientific research documents, whether they are published or not. The documents may come from teaching and research institutions in France or abroad, or from public or private research centers.

L'archive ouverte pluridisciplinaire **HAL**, est destinée au dépôt et à la diffusion de documents scientifiques de niveau recherche, publiés ou non, émanant des établissements d'enseignement et de recherche français ou étrangers, des laboratoires publics ou privés.

Emergence of coexistence and limit cycles in the chemostat model with flocculation for a general class of functional responses

R. Fekih-Salem[a,d,*], **A. Rapaport**[b,e], **T. Sari**[c,f]

[a] *Université de Tunis El Manar, ENIT, LAMSIN, BP 37, Le Belvédère, 1002 Tunis, Tunisie*
[b] *UMR INRA-SupAgro MISTEA, 2 p. Viala, 34060 Montpellier, France*
[c] *IRSTEA, UMR Itap, 361 rue Jean-François Breton, 34196 Montpellier France*
[d] *Université de Monastir, ISIMa, BP 49, Av Habib Bourguiba, 5111 Mahdia, Tunisie*
[e] *EPI INRA-INRIA MODEMIC, route des Lucioles, 06902 Sophia-Antipolis, France*
[f] *Université de Haute Alsace, LMIA, 4 rue des frères Lumière, 68093 Mulhouse, France*

Abstract

We consider a model of two microbial species in a chemostat competing for a single-resource, involving the flocculation of the most competitive species which is present in two forms: isolated and attached. We first show that the model with one species and a non-monotonic growth rate of isolated bacteria may exhibit bi-stability and allows the appearance of unstable limit cycles through a sub-critical Hopf bifurcations due to the joined effect of inhibition and flocculation. We then show that the model with two species presents an even richer set of possible behaviors: coexistence, bi-stability and occurrence of stable limit cycles through a super-critical Hopf bifurcations. All these features cannot occur in the classical chemostat model, where generically at most one competitor can survive on a single resource.

Keywords: Chemostat, Flocculation, Bi-stability, Coexistence, Hopf bifurcation, Limit cycle

1. Introduction

In the mathematical model of competition of n species for a single growth-limiting nutrient in a chemostat, a classical result, well-known as the *Competitive Exclusion Principle* (CEP), asserts that generically at most one species can survive to the competition [6, 9, 10, 22, 24, 27]. The dynamical equations of the model are

$$\begin{cases} \dot{S} &= D(S_{in} - S) - \displaystyle\sum_{i=1}^{n} \frac{1}{y_i} f_i(S) x_i, \\ \dot{x}_i &= [f_i(S) - D] x_i, \qquad\qquad i = 1, \dots, n \end{cases} \tag{1}$$

where $S(t)$ denotes the concentration of the substrate at time t, $x_i(t)$ denotes the concentration of the species i at time t and n represents the number of species. The operating parameters S_{in} and D denote, respectively, the concentration of the substrate in the feed device and the dilution rate of the chemostat. For $i = 1, \dots, n$, the function $f_i(\cdot)$ represents the per-capita growth rate of the species i (or its functional response) and y_i is the growth yield which can be chosen equal to one, without loss of generality.

Several extensions of this model have been studied in the literature. In [1], Butler and Wolkowicz have studied the model (1) for a general class of growth rates including monotonic and non-monotonic growth functions such as the Monod and Haldane laws. This last law takes into account the growth-limiting for low concentrations of substrate and the growth-inhibiting for high concentrations. For distinct break-even concentrations, they have demonstrated that the

*Corresponding author
Email addresses: radhouene.fs@gmail.com (**R. Fekih-Salem**), rapaport@supagro.inra.fr (**A. Rapaport**), tewfik.sari@irstea.fr (**T. Sari**)

competitive exclusion holds where at most one competitor avoids extinction. In some cases, the species that wins the competition depends on the initial condition. Extension with inhibition by reaction product has been also considered in [20].

Recently, Sari and Mazenc, in [24], were able to construct a Lyapunov function to study the global dynamics of the model (1) with a general class of growth rates, distinct removal rates for each species and variable yields, depending on the concentration of substrate. They showed that at most one competitor can survive, the one with the lowest break-even concentration, that is the species that consumes less substrate at steady state. Sari, in [22, 23], proposed a new Lyapunov function for the study of global asymptotic behavior of model (1), which is an extension of the Lyapunov functions used by Hsu [12] and by Wolkowicz and Lu [29].

However, the CEP contradicts the biodiversity that is observed, for instance in aquatic ecosystems where phytoplankton species competing for same resources can coexist (see [13, 25]). Such a biodiversity is also observed in laboratory, with mixed cultures including at least two competitors for a single resource (see [11, 26]).

To construct mathematical models that are more consistent with real-world observations, several improvements of the idealized model of competition have been proposed. Typically, adding terms of inter-specific competition between populations of microorganisms and/or intra-specific competition between individuals of the same species in the classical chemostat model leads to dynamics where species can coexist at the equilibrium, [3, 16, 30]. Recently, many papers in the literature have proposed extensions of the classical chemostat model that present periodic solutions or limit cycles due to impulsive effect [17, 32]. Study of predator-prey in the chemostat model with time delays and diffusion shows the existence of periodic solutions due to Hopf bifurcation [31].

In this paper, we consider a mechanism due to flocculation of bacteria and show how it can lead also to oscillations and non intuitive phenomena of the dynamics. This mechanism is different than the ones previously considered in the literature for explaining the oscillations that are observed experimentally. Indeed, understanding and exploiting the flocculation process appears to be a major challenge to tackle contemporary issues in the fields of wastewater treatments and development of renewable energy, and to improve next future bioprocesses. In [7], the effect of flocculation on the growth dynamics was analyzed with an arbitrary number of bacteria in flocs. Haegeman and Rapaport [8] proposed a competition model of two microbial species on a single nutrient with monotonic increasing uptake functions, where attached bacteria do not grow and are subject to the same dilution rate than isolated biomass. Assuming that the most competitive species inhibits its growth by the formation of flocs, they could explain the coexistence between two species. An extension of this model was studied in [4] without neglecting the substrate consumption of attached bacteria, but assuming that they consume less substrate than the isolated bacteria, since the bacteria at the surface of flocs have easier access to the substrate than the bacteria inside the flocs. More recently, Fekih-Salem et al. [2] proposed a model of flocculation of n species that generalizes several models [5, 14, 21, 28] that have been considered in the literature. Assuming that the flocculation and deflocculation dynamics are fast compared to the growth dynamics, Haegeman and Rapaport [8] could build a density-dependent model with the same dilution rate [18, 19]. Moreover, the study of a flocculation model [2] with different dilution rates leads also to density-dependent dilution rates for the overall biomass [2], which is a new feature. In the present work, we revisit the flocculation model proposed in [8], but considering that the attached bacteria consumes also the substrate. Moreover, we consider a general class of growth rates to study the effects on coexistence of two competitors, to be compared with the results obtained by Butler and Wolkowicz [1], where at most one competitor can survive on a single resource in absence of flocculation.

The paper is organized as follows. We first introduce in Section 2 the flocculation model (2) along with assumptions and preliminary results. In Section 3 the model is studied with only one species, non-monotonic growth rate of isolated bacteria and monotonic growth rate of aggregated bacteria. We show that this model can present unstable limit cycles through a sub-critical Hopf bifurcation. An analysis of the two species model is derived in Section 4 with a monotonic growth rate of the second species. The numerical simulations show the occurrence of stable limit cycles through a super-critical Hopf bifurcations. In Section 5, we study the particular case of the flocculation model where the non-monotonic growth rate of attached bacteria is directly related to the isolated ones. Finally, we draw conclusions in the last Section 6. The mathematical proofs are given in Appendix A and the parameter values used in simulations are provided in Appendix B.

2. Mathematical model

The model of two competitors on one resource in a chemostat, taking into account the flocculation of the most competitive species, can be written as follows

$$\begin{cases} \dot{S} &= D(S_{in} - S) - f(S)u - g(S)v - f_2(S)x_2 \\ \dot{u} &= f(S)u - au^2 + bv - Du \\ \dot{v} &= g(S)v + au^2 - bv - Dv \\ \dot{x}_2 &= f_2(S)x_2 - Dx_2 \end{cases} \tag{2}$$

where $u(t)$ and $v(t)$ denote, respectively, the concentration of isolated and attached bacteria of the first species at time t. Functions $f(\cdot)$ and $g(\cdot)$ represent, respectively, the per-capita growth rates of the isolated and attached bacteria. The variable $x_2(t)$ denotes the concentration of the second species and $f_2(\cdot)$ represents the per-capita growth rate of the second species. We assume that two isolated bacteria can stick together to form a new floc with rate a, and that a floc can split and liberate isolated bacteria with rate b. The growth rates satisfy the following assumptions:

H1: The function $f : \mathbb{R}_+ \to \mathbb{R}_+$ is continuously differentiable, $f(0) = 0$ and there exist two positive real numbers λ_0 and μ_0, such that $\lambda_0 < \mu_0$ and

$$\begin{cases} f(S) > D & \text{if} \quad S \in]\lambda_0, \mu_0[\\ f(S) < D & \text{if} \quad S \notin [\lambda_0, \mu_0]. \end{cases}$$

We shall allow λ_0 and/or μ_0 to be equal to $+\infty$, and our results can then be applied for any monotonic growth rate for the isolated bacteria.

H2: $g(0) = 0$ and $g'(S) > 0$ for all $S > 0$.

H3: $f_2(0) = 0$ and $f_2'(S) > 0$ for all $S > 0$.

When equations $g(S) = D$ and $f_2(S) = D$ have solutions, they are unique and we define the usual *break-even concentrations*

$$\lambda_1 = g^{-1}(D) \quad \text{and} \quad \lambda_2 = f_2^{-1}(D).$$

Otherwise, we put $\lambda_k = +\infty$ $(k = 1, 2)$. One has the following property.

Proposition 2.1. *For any non-negative initial condition, the forward solution of (2) remains non-negative and positively bounded. The set*

$$\Omega = \left\{(S, u, v, x_2) \in \mathbb{R}_+^4 : Z = S + u + v + x_2 = S_{in}\right\}$$

is positively invariant and is a global attractor for the dynamics (2).

In the following, we shall use for convenience the abbreviation LES for Locally Exponentially Stable equilibria.

3. Study of the one species model

In order to better understand the qualitative behaviors of trajectories of the flocculation model (2), we propose in this section to study first the one species case, that is the 3d model

$$\begin{cases} \dot{S} = D(S_{in} - S) - f(S)u - g(S)v \\ \dot{u} = f(S)u - au^2 + bv - Du \\ \dot{v} = g(S)v + au^2 - bv - Dv. \end{cases} \tag{3}$$

This study has led us to define several functions, given below, that are also useful for the analysis of the two species model studied in Section 4.

3.1. Existence of equilibria

The equilibria of (3) are given by the solutions of the following system

$$\begin{cases} D(S_{in} - S) &= f(S)u + g(S)v \\ 0 &= f(S)u - au^2 + bv - Du \\ 0 &= g(S)v + au^2 - bv - Dv. \end{cases} \tag{4}$$

At equilibrium, if $u = 0$ then one has necessarily $v = 0$ and vice versa. Thus, one cannot observe a steady state with extinction of isolated or attached bacteria only. Denote

$$\varphi(S) = f(S) - D \quad \text{and} \quad \psi(S) = g(S) - D.$$

The sum of the second and the third equation of (4) gives the following equation

$$\varphi(S)u + \psi(S)v = 0. \tag{5}$$

Under the assumptions **H1**-**H3**, three possible cases may arise:

$$\lambda_0 < \lambda_1 < \mu_0, \quad \lambda_0 < \mu_0 < \lambda_1 \quad \text{or} \quad \lambda_1 < \lambda_0 < \mu_0.$$

The latter case appears to be unrealistic from the biological point of view because the attached bacteria are expected to have a less easy access to substrate than the isolated bacteria (this access being proportional to the external surface of flocs). So, we shall consider only the two first possible cases in the following. Equation (5) has a positive solution (u, v) if and only if $\varphi(S)$ and $\psi(S)$ at steady state have opposite signs (see Fig. 1). Let I and J be the sets given in Table 1. If $\varphi(S) < 0$ and $\psi(S) > 0$, then S has to belong to the set I, and when $\varphi(S) > 0$ and $\psi(S) < 0$, S has to belong to the set J. Those conditions can be summarized by the single condition $S \in I \cup J$, with

$$I =]\lambda_0, \min(\mu_0, \lambda_1)[\quad \text{and} \quad J =]\max(\mu_0, \lambda_1), +\infty[. \tag{6}$$

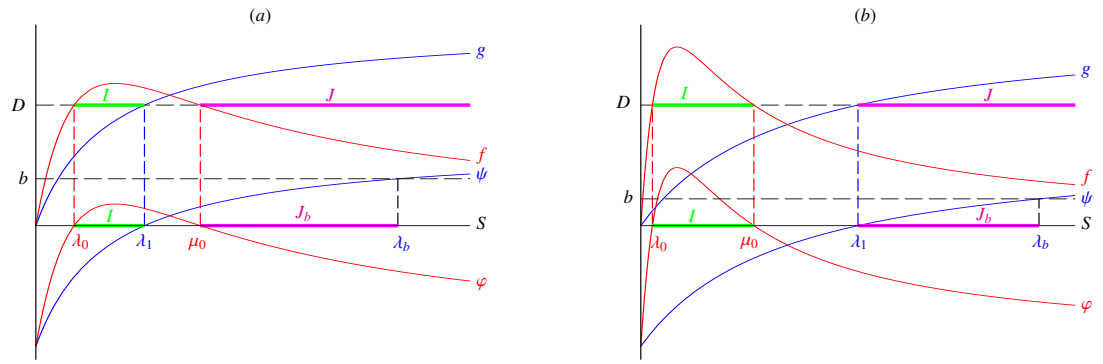

Figure 1: Growth function f of Haldane type and g of Monod type in two cases: $\lambda_1 < \mu_0$ and $\mu_0 < \lambda_1$. Intervals of existence of positive equilibria.

Case	I	J
$\lambda_1 < \mu_0$	$]\lambda_0, \lambda_1[$	$]\mu_0, +\infty[$
$\mu_0 < \lambda_1$	$]\lambda_0, \mu_0[$	$]\lambda_1, +\infty[$

Table 1: Intervals of existence of positive equilibria according to the case.

Then we have to seek solutions (S, u, v) of (4) with $S \in I \cup J$. As one has $\psi(S) \neq 0$, equation (5) can be rewritten as

$$v = -\frac{\varphi(S)}{\psi(S)}u. \tag{7}$$

Replacing v by its expression (7) in the second equation of (4), we obtain (for positive u, v)

$$u = U(S) \quad \text{with} \quad U(S) := \frac{\varphi(S)}{a\psi(S)}\left[\psi(S) - b\right]. \tag{8}$$

By replacing u by (8) in (7), we obtain

$$v = V(S) \quad \text{with} \quad V(S) := -\frac{\varphi^2(S)}{a\psi^2(S)}\left[\psi(S) - b\right]. \tag{9}$$

If the equation $\psi(S) = b$ has solution, it is unique and we set

$$\lambda_b = \psi^{-1}(b).$$

Otherwise, we let $\lambda_b = +\infty$. Note that u and v defined by (8) and (9), respectively, are positive if and only if

$$S \in I \cup J_b \quad \text{with} \quad J_b = J \cap [0, \lambda_b[.$$

We remark that the interval J_b is empty if $b < \psi(\mu_0)$ in the case $\lambda_1 < \mu_0$ (see Fig. 1(a)) and is empty if $b = 0$ in the case $\mu_0 < \lambda_1$ (see Fig. 1(b)). From (4), we deduce that $S_{in} - S = u + v$. Replacing u and v by (8) and (9), we obtain $S_{in} - S = H(S)$ where

$$H(S) := \frac{\varphi(S)}{a\psi^2(S)}\left[\psi(S) - b\right]\left[\psi(S) - \varphi(S)\right]. \tag{10}$$

We can then state the following result.

Proposition 3.1. *The system (3) has the following equilibria:*

1. *the washout equilibrium $E_0 = (S_{in}, 0, 0)$, that always exists.*
2. *a positive equilibrium $E_1 = \left(\bar{S}, \bar{u}, \bar{v}\right)$ with $\bar{S}$ solution of the equation $H(S) = S_{in} - S$, $\bar{u} = U(\bar{S})$, $\bar{v} = V(\bar{S})$, that exists if and only if $\bar{S} \in I \cup J_b$.*

A straightforward calculation gives the following expression of the derivative of $H(\cdot)$.

$$H' = f'\frac{(\psi - b)(\psi - 2\varphi)}{a\psi^2} + g'\varphi\frac{-\varphi\psi + 2\varphi(\psi - b) + b\psi}{a\psi^3} \tag{11}$$

whose sign can be positive or negative at $\bar{S} \in I \cup J_b$ (see Figs. 2 and 3). Moreover, the function $H(\cdot)$ is defined and positive on this interval. It vanishes at $\lambda_0, \mu_0, \lambda_b$ and tends to infinity as S tends to λ_1. We have obtained the following results.

Proposition 3.2.

- *If $S_{in} \leqslant \lambda_0$, then there is no positive equilibrium.*
- *If $\lambda_0 < S_{in} < \mu_0$ or $S_{in} > \lambda_b$, then there exists at least one positive equilibrium. Generically, there is an odd number of positive equilibria.*
- *If $\mu_0 < S_{in} < \lambda_b$, then the system has generically an even number of positive equilibria. In this case, there exists at least two positive equilibria if $\lambda_1 < \mu_0$, otherwise, the system can have no positive equilibrium.*

Fig. 2 illustrates the number of positive equilibria in the case $\lambda_1 < \mu_0$, depending on S_{in}, where the function $H(\cdot)$ is increasing (a) or non-monotonic (b) on I. $x_1 = u + v$ is the total biomass of the first species.

To illustrate the existence of three positive equilibria on I (see Fig. 2(c)), we have considered the parameter values given in Table B.4 with the growth rates $f(\cdot)$ of Haldane-type and $g(\cdot)$ of Monod-type:

$$f(S) = \frac{m_{11}S}{K_{11} + S + \frac{S^2}{K_i}} \quad \text{and} \quad g(S) = \frac{m_{12}S}{K_{12} + S}.$$

In Fig. 2(c), the line of equation $x_1 = S_{in} - S$ seems to be quasi-horizontal due to the scale differences on the axes. In the same manner, Fig. 3 illustrates the case $\mu_0 < \lambda_1$ where the function $H(\cdot)$ is decreasing (a) or non-monotonic (b) on J_b. In all figures, we have chosen the red color for LES equilibria, blue color for unstable equilibria and green color when an equilibrium can change its stability.

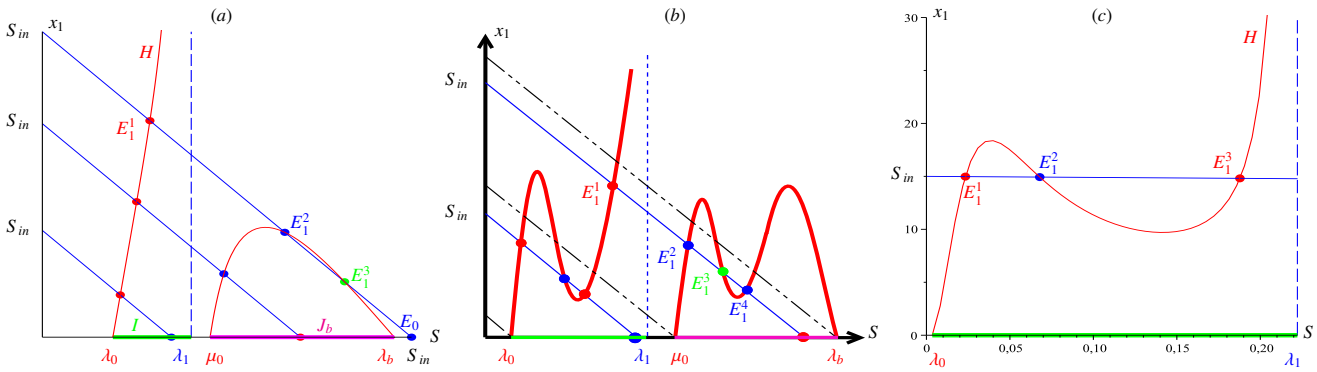

Figure 2: The case $\lambda_1 < \mu_0$: Multiplicity of positive equilibria: H is increasing (a) and non-monotonic (b) on I. (c) Numerical example of existence of three positive equilibria.

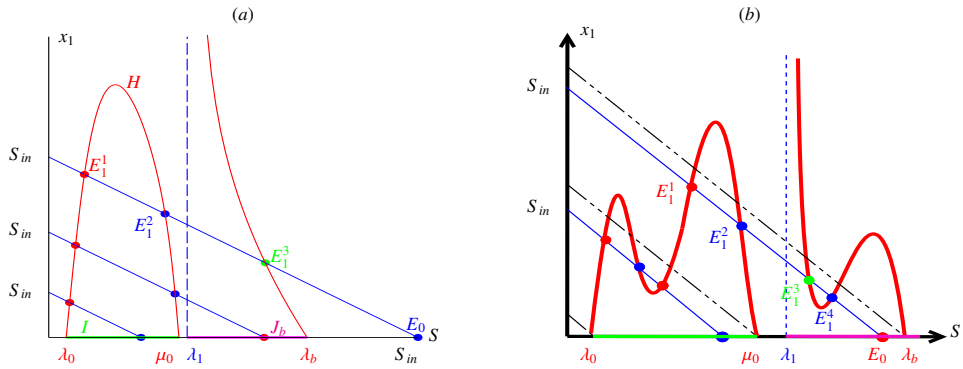

Figure 3: The case $\mu_0 < \lambda_1$: Multiplicity of positive equilibria: H is decreasing (a) and non-monotonic (b) on J_b.

3.2. *Stability of equilibria*

In the next Proposition, we give a condition for which the washout is the unique globally asymptotically stable equilibrium of (3). When this condition is not fulfilled, dynamics (3) admits multi-equilibria and we focus then on the study of their local asymptotic stability.

Proposition 3.3. *If $S_{in} < \lambda_0$, then the washout equilibrium E_0 is globally asymptotically stable for (3) with respect to initial conditions in $\mathbb{R}^3_+$.*

To study the local stability of each equilibrium point of dynamics (3), we consider the density of total mass in the chemostat $z = S + u + v$ and the vector $y = (S, u)'$. It is easy to see that system (3) possesses a cascade structure in the (z, y) coordinates:

$$\begin{cases} \dot{z} = D(S_{in} - z) \\ \dot{y} = \phi_2(z, y), \end{cases}$$

where

$$\phi_2(z, y) = \begin{bmatrix} D(S_{in} - S) - f(S)u - g(S)(z - S - u) \\ (f(S) - au - D)u + b(z - S - u) \end{bmatrix}.$$

Thus, the three order system (3) can be reduced to the two-dimensional system which is simply the projection on the plane (S, u)

$$\begin{cases} \dot{S} = D(S_{in} - S) - f(S)u - g(S)(S_{in} - S - u) \\ \dot{u} = (f(S) - au - D)u + b(S_{in} - S - u) \end{cases} \tag{12}$$

with $z = S_{in}$ the equilibrium of the first dynamics. Let A_1 denote the Jacobian matrix of reduced system (12) at the equilibrium $\mathbb{E}_1 = (\bar{S}, \bar{u})$ corresponding to the equilibrium E_1 of (3). We define

$$D_1(\bar{S}) := \det A_1 \quad \text{and} \quad T_1(\bar{S}) := \operatorname{tr} A_1.$$

We have proved the following results.

Proposition 3.4. *The washout equilibrium E_0 is LES if and only if $\varphi(S_{in}) < 0$ and $S_{in} < \lambda_b$.*

Proposition 3.5. *A positive equilibrium E_1 is LES if and only if*

$$\begin{cases} H'(\bar{S}) > -1 & & \text{if} \quad \bar{S} \in I \\ H'(\bar{S}) < -1 \quad \text{and} \quad T_1(\bar{S}) < 0 & & \text{if} \quad \bar{S} \in J_b. \end{cases} \tag{13}$$

We summarize these results in Table 2

Equilibria	Existence condition	Stability condition
E_0	always exists	$\varphi(S_{in}) < 0$ and $S_{in} < \lambda_b$
E_1	$H(S) = S_{in} - S$ has solution $\bar{S} \in I \cup J_b$	condition (13)

Table 2: Existence and local stability of equilibria of system (3).

3.3. Sub-critical Hopf bifurcation

When $\bar{S} \in J_b$, the equilibrium $\mathbb{E}_1$ can change its stability through a Hopf bifurcation. More precisely, when $H'(\bar{S}) < -1$, $T_1(\bar{S})$ can change its sign from positive to negative as S_{in} increases because $f(\cdot)$ is a non-monotonic function. Denote $\bar{S}_{in}$ the critical value of S_{in} for which the curve of the function $H(\cdot)$ is tangent to the line of equation $x_1 = S_{in} - S$. If $S_{in} \in]\lambda_b, \bar{S}_{in}[$, there exist a positive equilibrium denoted $\mathbb{E}_1^1$ that is LES, the washout equilibrium $\mathbb{E}_0$ and the positive equilibrium $\mathbb{E}_1^2$ that are unstable while the positive equilibrium $\mathbb{E}_1^3$ can change its stability (see Fig. 2(a)). In this case, $\mathbb{E}_1^3$ satisfies the condition $H'(\bar{S}) < -1$ whereas $T_1(\bar{S})$ can change its sign as S_{in} increases. Fig. 4(a) illustrates this change of sign of $T_1(\bar{S})$ where $D_1(\bar{S})$ is positive or, equivalently, $H'(\bar{S}) < -1$ from expression (A.6). In fact, the Jacobian matrix of reduced system (12) at $\mathbb{E}_1^3$ has one pair of complex-conjugate eigenvalues

$$\bar{\lambda}_j(S_{in}) = \alpha(S_{in}) \pm i\beta(S_{in}), \quad j = 1, 2$$

which becomes purely imaginary for a particular value $S_{in} = S_{in}^c$ such that $\alpha(S_{in}^c) = 0$, with $\beta(S_{in}^c) \neq 0$. One can check (numerically) that the following inequality is fulfilled

$$\frac{d\alpha}{dS_{in}}(S_{in}^c) > 0 \, .$$

With the values of the parameters given in Table B.4, we have first considered the two following values of the parameter S_{in}.

i. For $S_{in} = 9.8$, $\mathbb{E}_1^3$ is a stable focus since the Jacobian matrix has one pair of complex-conjugate eigenvalues with negative real part

$$\bar{\lambda}_{1,2} \simeq -0.003 \pm 0.259\, i \, .$$

ii. For $S_{in} = 9.95$, $\mathbb{E}_1^3$ changes behavior and becomes an unstable focus whose eigenvalues are given by

$$\bar{\lambda}_{1,2} \simeq 0.001 \pm 0.261\, i \, .$$

To better illustrate the change of asymptotic behavior of $\mathbb{E}_1^3$, we represent the variations of the eigenvalues as the parameter S_{in} increases from $S_{in} = 5$ to 14.5 (see Fig. 4(b)) where the pair of complex-conjugate eigenvalues crosses the imaginary axis at $S_{in}^c \simeq 9.911$ from negative half plane to positive half plane.

Note that the equilibria $\mathbb{E}_0$ and $\mathbb{E}_1^2$ are a saddle points in the Figs. 4(c) and 5(c). As the parameter S_{in} approaches its critical value, the region of attraction of $\mathbb{E}_1^3$ is bounded by the unstable cycle, which shrinks and disappears in a sub-critical Hopf bifurcation.

i. For $S_{in} = 9.8$, Fig. 5(c) shows the bi-stability in the plan (S, u) with convergence to stable focus $\mathbb{E}_1^3 \simeq (3.624, 3.565)$ or to stable node $\mathbb{E}_1^1 \simeq (0.561, 8.669)$: see on Fig. 5(a) the convergence (after a long transient of oscillations) to $\mathbb{E}_1^3$ (for the initial condition $S(0) = 3.5$ and $u(0) = 3.5$) and on Fig. 5(b) the convergence to $\mathbb{E}_1^1$ (for the initial condition $S(0) = 3.4$ and $u(0) = 3.6$).

ii. For $S_{in} = 9.95$, Fig. 4(c) shows the converge to the stable node $\mathbb{E}_1^1 \simeq (0.562, 8.8)$ for several positive initial conditions and $\mathbb{E}_1^3$ becomes an unstable focus.

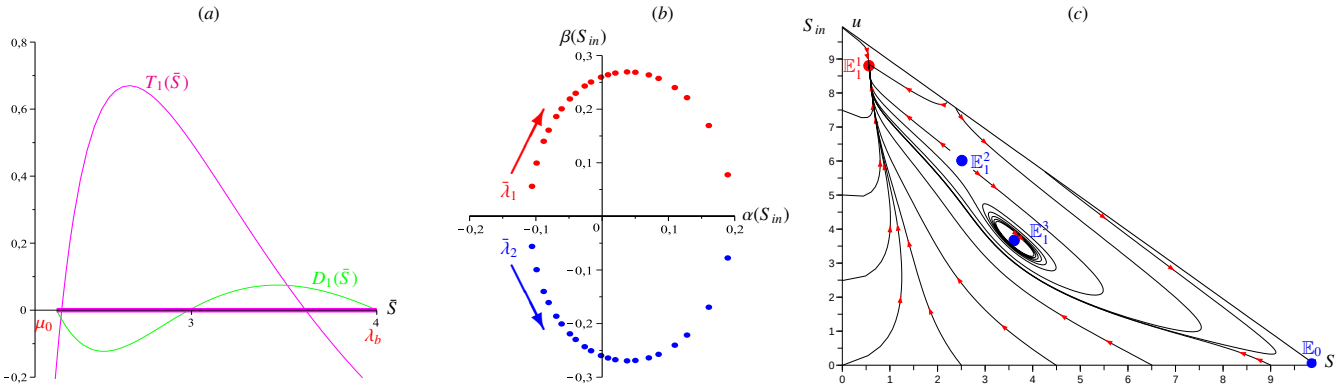

Figure 4: Sub-critical Hopf bifurcation: (a) change of sign of $T_1(\bar{S})$ where $D_1(\bar{S}) > 0$. (b) Variation of a pair of complex-conjugate eigenvalues as S_{in} increases. (c) The phase portrait of (12) for $S_{in} = 9.95$.

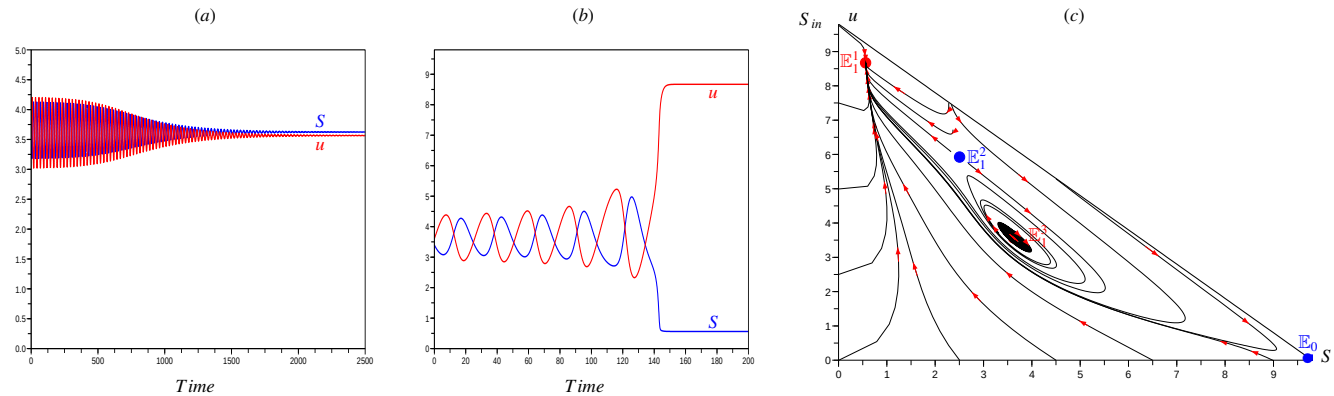

Figure 5: Bi-stability of $\mathbb{E}_1^3$ and $\mathbb{E}_1^1$ for $S_{in} = 9.8$.

We conclude that the one species model (3) with a non-monotonic functional response presents a richness of behaviors with possibly multiple positive equilibria, bi-stability and existence of unstable limit cycle resulting from a sub-critical Hopf bifurcation, all of them being not possible without flocculation. In the next section, we study the effects on the asymptotic behavior of system (2) when another species that does not aggregate and with monotonic growth is present.

4. Study of the two species model

In this section, we extend the previous analysis to the full model (2) with two species.

4.1. Existence and local stability of equilibria

Under the assumptions **H1**-**H3**, we have proved the following result:

Proposition 4.1. *The system (2) admits the following equilibria:*

1. *The washout equilibrium $F_0 = (S_{in}, 0, 0, 0)$, that always exists.*
2. *The equilibrium $F_2 = (\lambda_2, 0, 0, S_{in} - \lambda_2)$ of extinction of species 1, that exists if and only if $\lambda_2 < S_{in}$.*
3. *One or more equilibria $F_1 = (\bar{S}, \bar{u}, \bar{v}, 0)$ of extinction of species 2, where $\bar{S}$ is solution of the equation $H(S) = S_{in} - S$, $\bar{u} = U(\bar{S})$, $v = V(\bar{S})$, that exist if and only if $\bar{S} \in I \cup J_b$.*
4. *The positive equilibrium $F^* = \left(\lambda_2, u^*, v^*, x_2^*\right)$ with $u^* = U(\lambda_2)$, $v^* = V(\lambda_2)$, $x_2^* = S_{in} - \lambda_2 - H(\lambda_2)$, that exists if and only if $\lambda_2 \in I \cup J_b$ and $S_{in} - \lambda_2 > H(\lambda_2)$,*

where the function $U(\cdot)$, $V(\cdot)$ and $H(\cdot)$ are defined in (8), (9) and (10).

As for the study of the one species model, a change of coordinates that reveals a cascade structure of the dynamical system is convenient for the stability analysis. We consider the total mass density $Z = S + u + v + x_2$ and the vector $Y = (S, u, x_2)'$. The system (2) is then equivalent to the system

$$\begin{cases} \dot{Z} = D(S_{in} - Z) \\ \dot{Y} = \phi_3(Z, Y), \end{cases}$$

where

$$\phi_3(Z, Y) = \begin{bmatrix} D(S_{in} - S) - f(S)u - g(S)(Z - S - u - x_2) - f_2(S)x_2 \\ [f(S) - au - D]\, u + b\,(Z - S - u - x_2) \\ [f_2(S) - D]\, x_2 \end{bmatrix}.$$

Thus, the fourth-order system (2) can be reduced to the three order system which is simply the projection on the three-dimensional space (S, u, x_2)

$$\begin{cases} \dot{S} = D(S_{in} - S) - f(S)u - g(S)(S_{in} - S - u - x_2) - f_2(S)x_2 \\ \dot{u} = [f(S) - au - D]\, u + b\,(S_{in} - S - u - x_2) \\ \dot{x}_2 = [f_2(S) - D]\, x_2 \end{cases} \tag{14}$$

with $Z = S_{in}$. Our results about the local stability conditions of the equilibria F_0, F_1 and F_2 are summarized in the following proposition:

Proposition 4.2.

1. *F_0 is LES if and only if $\varphi(S_{in}) < 0$ and $S_{in} < \min(\lambda_b, \lambda_2)$.*
2. *F_2 is LES if and only if $\varphi(\lambda_2) < 0$ and $\lambda_2 < \lambda_b$.*
3. *F_1 is LES if and only if $\bar{S} < \lambda_2$ and the condition (13) is satisfied.*

Thus we find the stability condition of the one species model (3) and when $\bar{S} < \lambda_2$ it recalls the CEP where the species that consumes less substrate at steady state wins the competition in the classical chemostat model. The next proposition gives sufficient conditions for the stability or instability of the positive equilibrium $F^* = (\lambda_2, u^*, v^*, x_2^*)$, depending on the break-even concentration λ_2.

Proposition 4.3.

1. *When $\lambda_2 \in I$, F^* is LES if $H'(\lambda_2) > -1$.*
2. *When $\lambda_2 \in J_b$, F^* is always unstable.*

Note that if $\lambda_2 \in I$ and $H'(\lambda_2) < -1$, then F^* can be stable or unstable as it will be illustrated in Section 4.2 . We summarize the results of this section in Table 3.

The result of Prop. 4.3 is illustrated on Fig. 6, with the existence of a unique positive equilibrium F^* when $\lambda_1 < \mu_0$. On this figure, one can see that there are three equilibria F_1, that we denote F_1^k with $k = 1, 2, 3$.

- when $\lambda_2 \in I$ (case a), F^* is LES and all the equilibria F_1^1, F_1^2, F_1^3, F_2 and F_0 are unstable. Numerical simulations show the global convergence towards the coexistence equilibrium F^* from any positive initial condition.

- when $\lambda_2 \in J_b$ (case b), F^* is unstable as F_1^2, F_1^3 and F_0 while F_1^1 and F_2 are LES. Numerical simulations show a bi-stability with convergence either to F_1^1 (and consequently the exclusion of the second species) or to F_2 (and consequently the exclusion of the first species).

Equilibria	Existence condition	Stability condition
F_0	always exists	$\varphi(S_{in}) < 0$ and $S_{in} < \min(\lambda_b, \lambda_2)$
F_2	$S_{in} > \lambda_2$	$\varphi(\lambda_2) < 0$ and $\lambda_2 < \lambda_b$
F_1	$H(S) = S_{in} - S$ has solution $\bar{S} \in I \cup J_b$	$\bar{S} < \lambda_2$ and condition (13)
F^*	$\lambda_2 \in I \cup J_b$ and $S_{in} - \lambda_2 > H(\lambda_2)$	$\lambda_2 \in I$ and Routh-Hurwitz condition (A.10)

Table 3: Existence and local stability of equilibria of system (2).

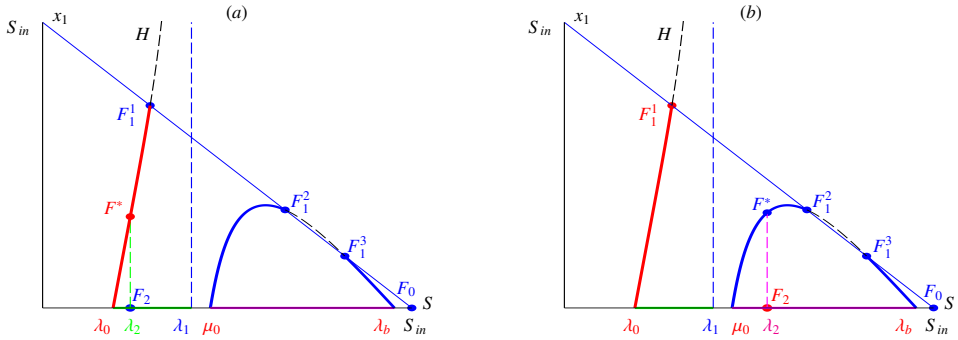

Figure 6: When $\lambda_1 < \mu_0$: Case a: $\lambda_2 \in I$; Case b: $\lambda_2 \in J_b$.

4.2. *Occurrence of limit cycles*

In the following, we focus on the change of stability of the positive equilibrium F^* through a Hopf bifurcation. More precisely, we analyze the bifurcations according to the parameters m_2 and S_{in}, when the conditions $\mu_0 < \lambda_1$, $\lambda_2 \in I$ and $H'(\lambda_2) < -1$ are satisfied (since the conditions of the Routh-Hurwitz criterion (A.10) are not fulfilled). To illustrate the Hopf bifurcation, we consider the same growth rates $f(\cdot)$ and $g(\cdot)$ for the first species than in Section 3, and for the second species we consider a growth rate $f_2(\cdot)$ of Monod-type

$$f_2(S) = \frac{m_2 S}{K_2 + S},$$

where m_2 is the maximum growth rate and K_2 the Michaelis-Menten constant. All the values of the parameters required for the simulation are given in Table B.5. Recall from the previous section that $\bar{S}_{in}$ denotes the critical value of S_{in} for which the graph of the function $H(\cdot)$ is tangent to the graph of the line $S \mapsto S_{in} - S$. We distinguish two main cases depending on the position of S_{in} relatively to this critical value.

4.2.1. *Pictures when $S_{in} \in]\mu_0, \bar{S}_{in}[$.*

Depending on the value λ_2, the break-even concentration of the second species, the following change of stability occur

- For $\lambda_2 \in]\lambda_0, \bar{S}_1[$, the equilibria F_0, F_2, F_1^1 and F_1^2 are unstable and F^* is LES (see Fig. 7(a)).
- For $\lambda_2 = \bar{S}_1$, F^* coalesces with F_1^1.
- For $\lambda_2 \in]\bar{S}_1, \bar{S}_2[$, F^* disappears in a saddle-node bifurcation and transfers stability to F_1^1.
- For $\lambda_2 = \bar{S}_2$, F_1^2 coalesces with F^*.
- For $\lambda_2 \in]\bar{S}_2, \lambda_2^{c_1}[$, F^* is unstable.
- For $\lambda_2 \in]\lambda_2^{c_1}, \mu_0[$, F^* is LES.

The Jacobian matrix of reduced system (14) at the equilibrium $\mathbb{F}^* = (\lambda_2, u^*, x_2^*)$ has one negative eigenvalue and one pair of complex-conjugate eigenvalues

$$\bar{\lambda}_j(m_2) = \alpha(m_2) \pm i\beta(m_2), \quad j = 1, 2$$

which becomes purely imaginary for a particular value $m_2 = m_2^{c_1}$ such that $\alpha(m_2^{c_1}) = 0$ with $\beta(m_2^{c_1}) \neq 0$. One can check (numerically) that the following inequality is fulfilled

$$\frac{d\alpha}{dm_2}(m_2^{c_1}) > 0 \, .$$

We have first considered numerically the two following cases.

- For $m_2 = 1.78$ (then one has $\lambda_2 \simeq 2.045$) and $S_{in} < \bar{S}_{in} \simeq 3.61$, F^* is a saddle-focus on the blue curve since the Jacobian matrix has one negative eigenvalue and one pair of complex-conjugate eigenvalues with positive real part

$$\bar{\lambda}_3 \simeq -4.875 \quad \text{and} \quad \bar{\lambda}_{1,2} \simeq 0.0012 \pm 0.0556\, i \, .$$

- For $m_2 = 1.7$ (then one has $\lambda_2 = 2.25$), F^* changes its stability and becomes a stable focus. The eigenvalues are given by

$$\bar{\lambda}_3 \simeq -4.015 \quad \text{and} \quad \bar{\lambda}_{1,2} \simeq -0.0251 \pm 0.0552\, i \, .$$

To better illustrate the change of stability of the positive equilibrium F^*, we have drawn the variations of the eigenvalues as m_2 increases (see Fig. 7(b)) where the pair of complex-conjugate eigenvalues crosses the imaginary axis at $m_2^{c_1} \simeq 1.775$ from negative half plane to positive half plane. Fig. 7(c) gives the corresponding real part of the complex-conjugate eigenvalues.

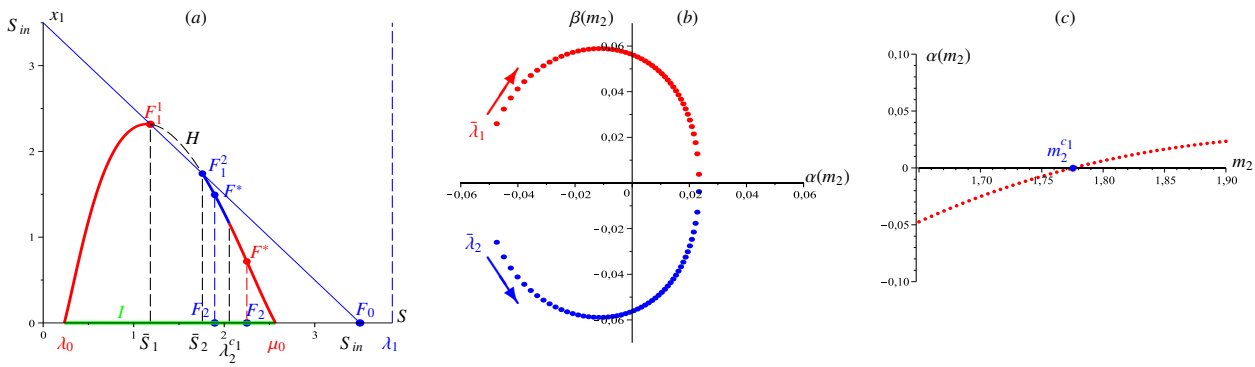

Figure 7: (a) Change of stability: F^* is LES on the red curve and unstable on the blue curve. Variation of a pair of complex-conjugate eigenvalues (b) and the corresponding real part (c) as m_2 increases.

Fig. 8 shows the ω-limit set projected in coordinates S, x_1 and x_2 depending on the value of the parameter m_2, which shows the existence of a limit cycle for a certain range of the values of m_2.

Finally, one has the following possible pictures.

1. For $m_2 < m_2^{c_1}$, the trajectories converge to the stable focus F^* or to the stable node F_1^1: Fig. 9(a) shows the bi-stability in three dimensions for $m_2 = 1.7$, with either convergence to $F^* \simeq (2.25, 0.492, 0.225, 0.533)$ or $F_1^1 \simeq (1.184, 1.163, 1.152, 0)$.
2. For $m_2^{c_1} < m_2 < m_2^{c_2} \simeq 1.790$, F^* changes its stability and becomes a saddle-focus with a super-critical Hopf bifurcation: Fig. 9(b) shows the bi-stability with two basins of attraction for $m_2 = 1.78$, one to the limit cycle and the other one to the stable node F_1^1. Thus, the trajectories converge to a limit cycle whose radius increases with respect to m_2, until the critical value $m_2^{c_2}$ when the limit cycle crosses the saddle point F_1^2 with a *Andronov-Leontovich or homoclinic bifurcation* [15].
3. For $m_2 > m_2^{c_2}$, all trajectories converge to the stable node F_1^1 where there is competitive exclusion of the second species: Fig. 9(c) shows for $m_2 = 1.792$ the convergence to the equilibrium F_1^1 from any positive initial condition.

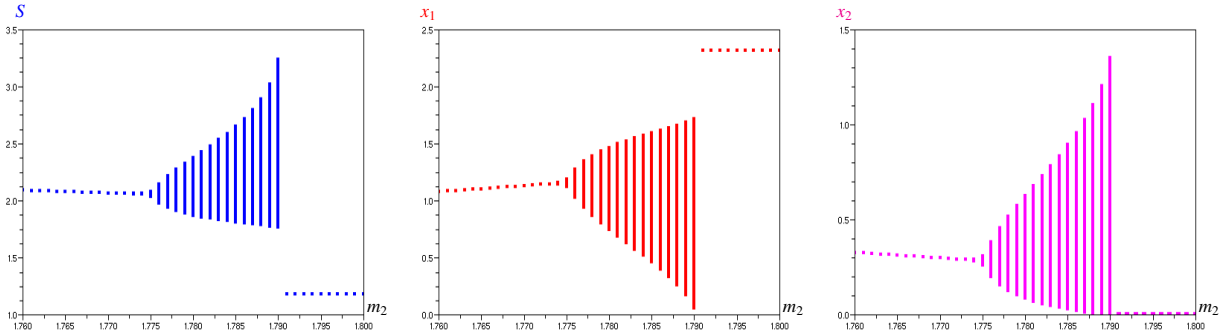

Figure 8: Projections of the ω-limit set in variables S, x_1 and x_2, as a function of m_2, reveal the occurrence of limit cycles through a super-critical Hopf bifurcation and disappearance through a homoclinic bifurcation.

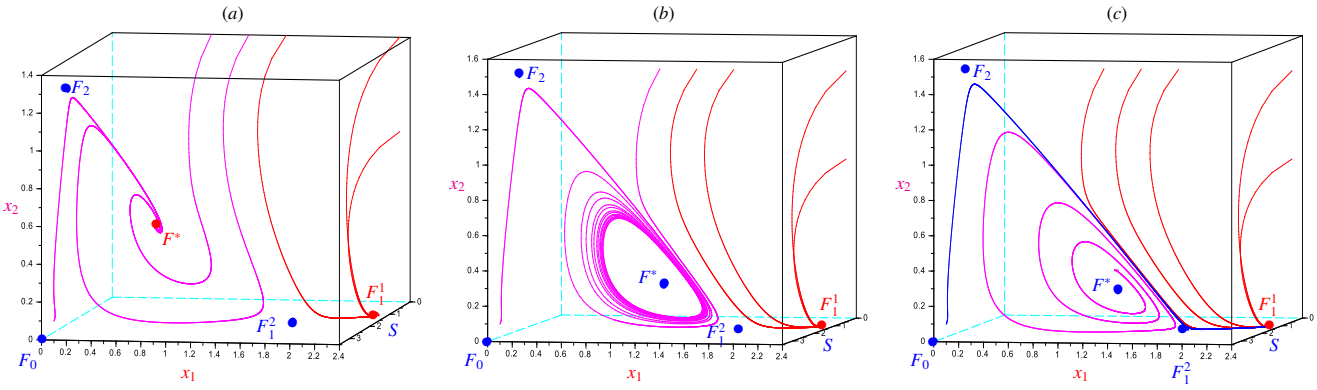

Figure 9: Super-critical Hopf bifurcation and homoclinic bifurcation: bi-stability, coexistence and limit cycle.

4.2.2. Pictures when $S_{in} > \bar{S}_{in}$.

Depending on the value of λ_2, one has the following change of stability.

- For $\lambda_2 \in]\lambda_0, \lambda_2^{c_2}[$, the equilibria F_0, F_2 are unstable whereas the equilibrium F^* is LES (see Fig. 10(a)).
- For $\lambda_2 \in]\lambda_2^{c_2}, \lambda_2^{c_1}[$, F^* is unstable.
- For $\lambda_2 \in]\lambda_2^{c_1}, \mu_0[$, F^* is LES.

The Jacobian matrix of reduced system (14) at the equilibrium $\mathbb{F}^* = (\lambda_2, u^*, x_2^*)$ has one negative eigenvalue and one pair of complex-conjugate eigenvalues that crosses the imaginary axis at $m_2^{c_1} \simeq 1.864$ from negative half plane to positive half plane as m_2 increases. Then it returns to the negative half plane by crossing the imaginary axis at $m_2^{c_2} \simeq 2.085$ (see Fig. 10(b)). Fig. 10(c) illustrates the corresponding real part of the complex-conjugate eigenvalues, as a function of m_2.

Fig. 11 illustrates the ω-limit set of the trajectories depending on the parameter m_2, projected on the axes S, x_1 and x_2.

Finally, the following possible pictures occur.

1. For $m_2 < m_2^{c_1}$, all solutions of (2) converge to the stable focus F^*. Fig. 12(a) shows the global convergence to $F^* \simeq (2, 0.757, 0.524, 0.37)$ in three dimensions for $m_2 = 1.8$, where F_0 and F_2 are unstable.
2. For $m_2 \in]m_2^{c_1}, m_2^{c_2}[$, there is a super-critical Hopf bifurcation with appearance of limit cycles where F^* becomes a saddle-focus. Fig. 12(b) shows the convergence to a limit cycle from any positive initial condition when $m_2 = 1.95$, for which $F^* \simeq (1.714, 0.970, 0.844, 0.121)$ is a saddle-focus and F_0 and F_2 are unstable. Fig. 12(c) shows the oscillatory coexistence with constant amplitude and frequency over the time. As m_2 increases, the size of the limit cycle get greater, then shrinks and finally disappears in a second super-critical Hopf bifurcation.
3. For $m_2 > m_2^{c_2}$, the equilibrium F^* returns to be a stable focus and one has the global convergence towards the coexistence of two species from any positive initial condition.

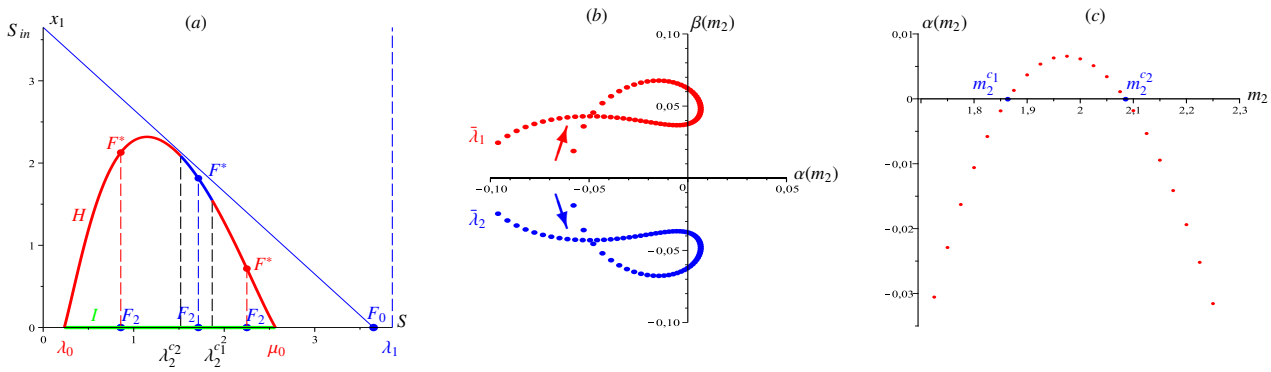

Figure 10: (a) Change of asymptotic behavior for $S_{in} > \bar{S}_{in}$ and $\lambda_2 \in I$. Double super-critical Hopf bifurcation: Variation of a pair of complex-conjugate eigenvalues (b) and the corresponding real part (c) as m_2 increases.

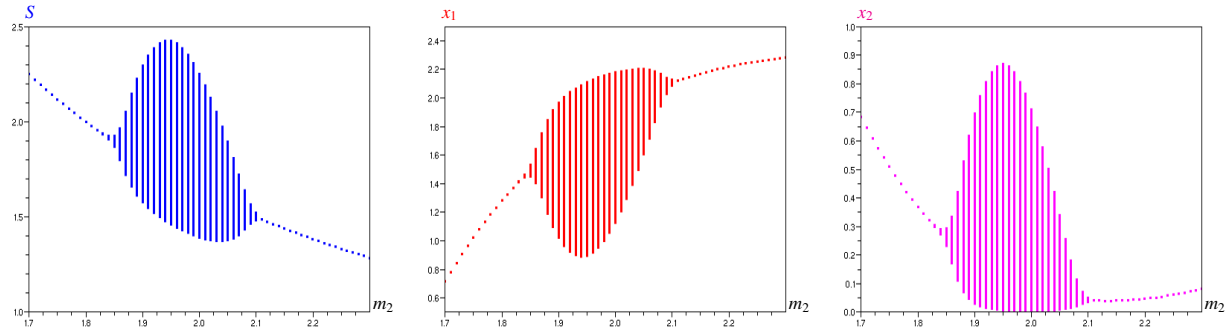

Figure 11: Projections of the ω-limit set in coordinates S, x_1 and x_2 depending on m_2: Occurrence and disappearance of limit cycles through a double super-critical Hopf bifurcation.

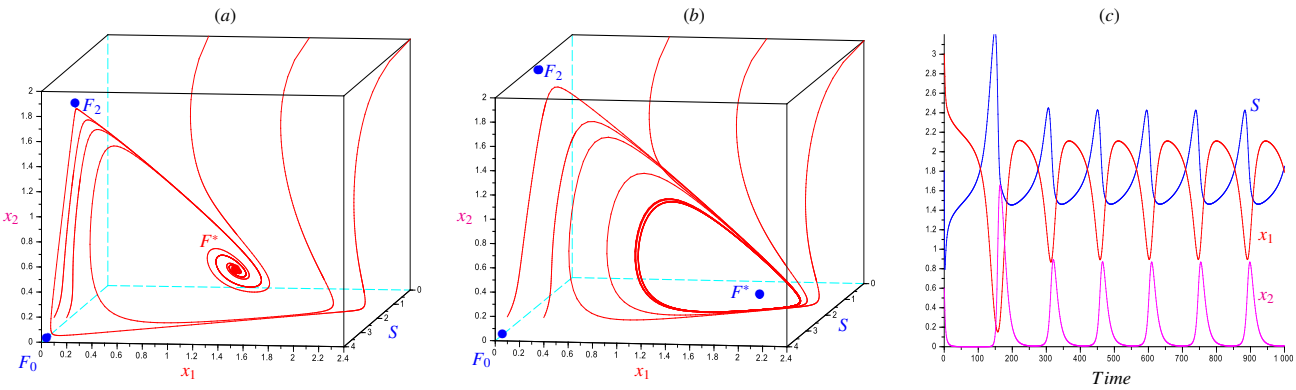

Figure 12: Coexistence: global convergence to the positive equilibrium F^* or to the limit cycle.

Fig. 13 shows the appearance and disappearance of limit cycles in the three-dimensional space (S, x_1, x_2) through a double super-critical Hopf bifurcation for different values of m_2. One can observe the following behaviors.

- For $m_2 = 1.83$, all trajectories converge to F^*.
- For $m_2 = 1.875$, all trajectories converge to a limit cycle whose size becomes greater until the parameter m_2 reaches the value $m_2 = 1.95$.
- For $m_2 = 2.05$, the limit cycle shrinks.
- For $m_2 = 2.1$, the second Hopf bifurcation occurs when F^* changes its stability and becomes a stable focus. Then, all trajectories converge to F^* from any positive initial condition.

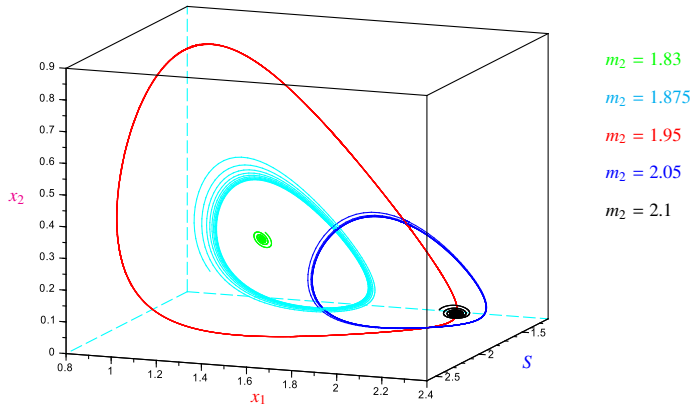

Figure 13: Occurrence and disappearance of limit cycles in the three-dimensional space (S, x_1, x_2) for different values of m_2.

5. Correlated growth rates of isolated and attached bacteria

In this section, we investigate the particular case of isolated and attached bacteria growth rates that are correlated in a specific way: we consider that the growth rate of attached bacteria is the same than the isolated one but for a modified substrate concentration that can be interpreted as an "apparent" substrate concentration for the attached biomass:

$$g(S) = f(pS)$$

where p is a parameter that belongs to $]0, 1]$. The modified concentration pS represents the proportion of the substrate that is accessible or "apparent" for the attached biomass. The multiplicative parameter p measures the effect of being attached depending for a given bacteria strain. Such a modeling consideration is motivated

1. by the fact that the nutrient access is less easy for the attached bacteria compared to isolated ones,
2. by a choice of distinguishing isolated and attached bacteria growth rates with a single parameter p,
3. by a way to obtain the model (2) from a continuous transformation of the classical chemostat model (1) that do not distinguish isolated and attached bacteria (when p is equal to one).

Our objective is to focus on the bifurcations related to the parameter p, under Assumptions **H1** and **H3**. One has

$$\lambda_1 = \frac{\lambda_0}{p} \quad \text{and} \quad \mu_1 = \frac{\mu_0}{p}$$

that verify $g(\lambda_1) = g(\mu_1) = D$. Hence, the inequalities $\lambda_0 < \lambda_1$, $\mu_0 < \mu_1$ and $\lambda_1 < \mu_1$ are fulfilled. Consequently, there are two possible cases

$$\lambda_0 < \lambda_1 < \mu_0 < \mu_1 \quad \text{or} \quad \lambda_0 < \mu_0 < \lambda_1 < \mu_1.$$

Generically, equation $\psi(S) = b$ has two positive solutions λ_b and μ_b (with $\lambda_b < \mu_b$) or no solution and we then put $\lambda_b = +\infty$ and $\mu_b = +\infty$. Consider the interval I defined in (6) and define

$$J_b = J \cap (]0, \lambda_b[\cup]\mu_b, +\infty[) \quad \text{where} \quad J =]\max(\mu_0, \lambda_1), \mu_1[.$$

Note that the interval J_b is empty if $b = 0$ in both cases. Moreover, the function $H(\cdot)$ is defined and positive on the interval $I \cup J_b$. It vanishes at λ_0, μ_0, λ_b and μ_b, and tends to infinity as S tends to λ_1 or μ_1. Fig. 14(a) illustrates the interval of existence of equilibria F_1 and F^* for the case $\lambda_1 < \mu_0$. Fig. 14(b) shows the existence of a unique positive equilibrium F^* which is LES on the red curve, while F_0, F_2, F_1^1, F_1^2, F_1^3 and F_1^4 are unstable. On the blue curve, F^* exists and is unstable like F_0, F_1^2, F_1^3 and F_1^4 while F_2 and F_1^1 are LES.

As p increases to 1, the curves $f(\cdot)$ and $g(\cdot)$ coalesce and the graph of the curve H on I and J_b converges to the graphs of $S = \lambda_0$ and $S = \mu_0$, respectively. Moreover, the positive equilibrium F^* disappears with a saddle-node bifurcation with F_1^1, which becomes LES when F_1^3 and F_1^4 disappear. For $p = 1$, F_1^1 is LES while F_1^2, F_2 and F_0 are

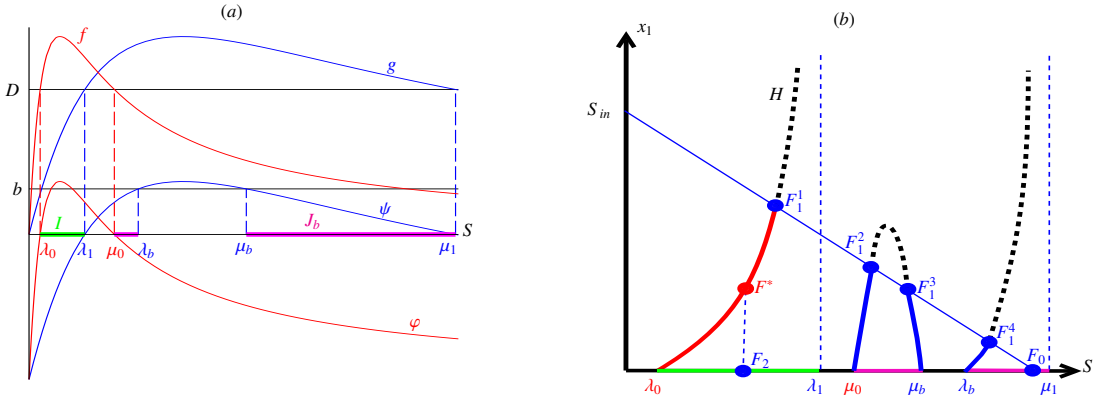

Figure 14: (a) Interval of existence of equilibria F_1 and F^* in the case $\lambda_1 < \mu_0$. (b) Existence of a unique positive equilibrium F^*.

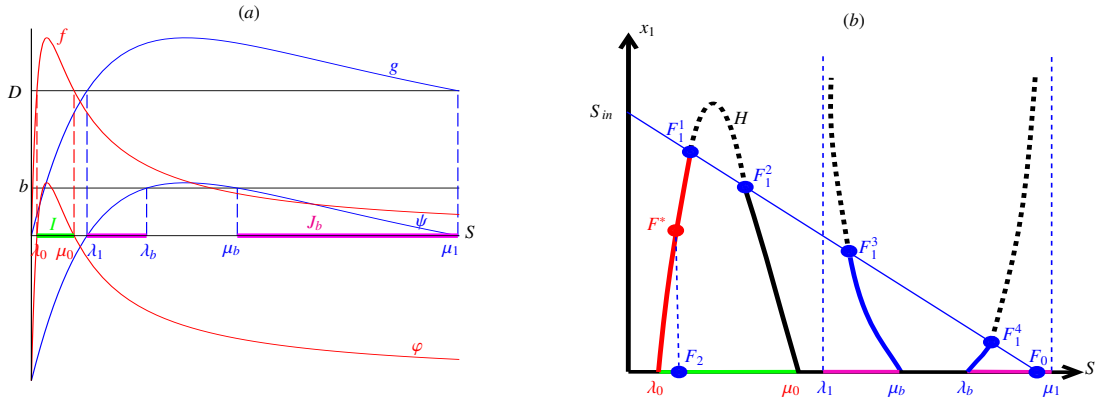

Figure 15: (a) Interval of existence of equilibria F_1 and F^* in the case $\mu_0 < \lambda_1$. (b) Existence of a unique positive equilibrium F^*.

unstable if $\lambda_2 \in]\lambda_0, \mu_0[$. Then, the system exhibits a bi-stability of F_1^1 and F_2 when $\lambda_2 > \mu_0$. Finally, we find the same result than for the classical chemostat model with a non-monotonic growth rate [1], where the system may exhibit bi-stability and (generically) at most one species wins the competition according to the initial condition.

Fig. 15(a) illustrates the interval of existence of equilibria F_1 and F^* in the case $\mu_0 < \lambda_1$. Fig. 15(b) shows the existence of a unique positive equilibrium F^* which is LES on the red curve, while F_0, F_2, F_1^1, F_1^2, F_1^3 and F_1^4 are unstable. On the black curve, F^* exists and can change its stability with the occurrence of a limit cycle where F_0, F_2, F_1^2, F_1^3 and F_1^4 are unstable while F_1^1 is LES. On the blue curve, F^* exists and is unstable as F_0, F_1^2, F_1^3 and F_1^4 while F_2 and F_1^1 are LES.

We conclude that making the parameter p varying from one to zero, the coexistence equilibrium can appear to be LES while all the other equilibria are unstable, which show that even under the stronger assumption of isolated and attached bacteria growth rates being correlated, the flocculation phenomenon can inhibit the growth of the most competitive species and allow then another species to coexist.

6. Discussion and conclusion

In this work, we have investigated mathematically and through numerical simulations a model of competition of two species when one of them flocculates, considering general classes of growth functions.

In a first step, we have studied this model when the species that do not flocculate is absent. We have shown the multiplicity of positive equilibria with the possibility of bi-stability of two positive equilibria. This first result is new and non intuitive: it cannot occur in the classical chemostat model (1) even with a non-monotonic growth rate (in this case, the system may exhibit a bi-stability but with at most one positive equilibrium, the other equilibrium

being the washout). Here, the proposed flocculation phenomenon allows to avoid the attraction basin of the washout equilibrium and consequently prevent the species extinction. Flocculation has thus an effect of "protection" of the species. Moreover and even more surprisingly, flocculation and substrate inhibition together allow the occurrence of an unstable limit cycle through a sub-critical Hopf bifurcations.

Our mathematical analysis of the complete two species model has revealed even richer possible behaviors. We have first shown the existence of a unique positive equilibrium that may be locally exponentially stable while all other equilibria are unstable. Then, the study of bifurcations according to the concentration of substrate in the feed bottle and the maximum growth rate of the second species shows the appearance of stable limit cycles due to Hopf bifurcations and the disappearance through homoclinic bifurcations. Numerical simulations show that the system may exhibit bi-stability with convergence either to a limit cycle or to the exclusion of the second species. In some cases, a coexistence exists about either a (locally exponentially) stable positive equilibrium or a limit cycle, depending on the initial condition. We deduce that the flocculation mechanism could be responsible of a coexistence, and moreover that a growth inhibition of the most competitive species could lead to the occurrence of limit cycles with coexistence of species.

Appendix A. Proofs

Proof of Prop. 2.1. One has

$$\begin{aligned} S = 0 \;&\Rightarrow\; \dot{S} = DS_{in} > 0\,, \\ v = 0 \;&\Rightarrow\; \dot{v} = au^2 \geqslant 0\,, \\ x_2 = 0 \;&\Rightarrow\; \dot{x}_2 = 0\,. \end{aligned}$$

Hence $S(t) \geqslant 0$, $v(t) \geqslant 0$ and $x_2(t) \geqslant 0$ for all $t \geqslant 0$. One has also

$$u = 0 \;\Rightarrow\; \dot{u} = bv \geqslant 0\,,$$

and then $u(t) \geqslant 0$ for all $t \geqslant 0$.

Let $Z = S + u + v + x_2$. One obtain from (2) $\dot{Z} = D(S_{in} - Z)$ and thus the explicit solution

$$Z(t) = S_{in} + (Z(0) - S_{in})e^{-Dt}. \tag{A.1}$$

One can write

$$Z(t) \leqslant \max(S_{in}, Z(0)) \quad \text{for all} \quad t \geqslant 0.$$

Therefore, the solution of (2) is positively bounded and is defined for all $t \geqslant 0$. From (A.1), it can be deduced that the set Ω is positively invariant and is a global attractor for (2). ■

Proof of Prop. 3.3. If $(u + v)(0) > 0$, then from the first equation of (3), we deduce that the solution $S(t)$ enters and remains in $[0, S_{in}]$ in a finite time T. For $t > T$, one has $S(t) \in [0, S_{in}]$ and therefore

$$\max(f(S(t)), g(S(t))) \leqslant \alpha$$

where $\alpha = \max(f(S_{in}), g(S_{in}))$. We recall that $\lambda_0 < \lambda_1$. For $S_{in} < \lambda_0$, we deduce that $\alpha < D$. Thus,

$$\frac{d(u+v)}{dt} = f(S)u + g(S)v - Du - Dv \leqslant (\alpha - D)(u + v).$$

It follows that $u + v$ converges to 0. From (A.1), we conclude that $z = S + u + v$ converges to S_{in}. This completes the proof. ■

Let A be the Jacobian matrix of (12) at (S, u), that we write with the following notation

$$A = \begin{bmatrix} -a_{11} & -a_{12} \\ a_{21} & -m_{22} \end{bmatrix} \tag{A.2}$$

with

$$a_{11} = -\psi(S) + f'(S)u + g'(S)(S_{in} - S - u), \quad a_{12} = f(S) - g(S), \quad a_{21} = f'(S)u - b, \quad m_{22} = -\varphi(S) + 2au + b.$$

In the following, we denote $\mathbb{E}$ or $\mathbb{F}$ the equilibriums of the reduced systems associated to equilibriums E or F of the full dynamics.

Proof of Prop. 3.4. At washout $E_0 = (S_{in}, 0, 0)$, we have $\bar{z} = S_{in}$, that is a globally exponentially equilibrium of the z sub-system.

Thus, it suffices to prove that $\mathbb{E}_0 = (S_{in}, 0)$ is a LES equilibrium of the reduced system (12). From (A.2), the Jacobian matrix of (12) at $\mathbb{E}_0$ is given by

$$A_0 = \begin{bmatrix} \psi(S_{in}) & \psi(S_{in}) - \varphi(S_{in}) \\ -b & \varphi(S_{in}) - b \end{bmatrix}.$$

Hence,

$$\operatorname{tr} A_0 = [\psi(S_{in}) - b] + \varphi(S_{in}), \quad \det A_0 = [\psi(S_{in}) - b]\varphi(S_{in}).$$

Thus, the two eigenvalues of A_0 are $\psi(S_{in}) - b$ and $\varphi(S_{in})$. They are negative, that is, E_0 is a stable node if and only if $S_{in} < \lambda_b$ and $\varphi(S_{in}) < 0$. This completes the proof. ■

Proof of Prop. 3.5. At the equilibrium $E_1 = (\bar{S}, \bar{u}, \bar{v})$, it is easy to see from Prop. 3.1 that $\bar{z} = \bar{S} + \bar{u} + \bar{v} = S_{in}$. Then it suffices to prove that $\mathbb{E}_1 = (\bar{S}, \bar{u})$ is a LES equilibrium of the reduced system (12). From expression (A.2) evaluated at $\mathbb{E}_1$, $D_1(\bar{S}) := \det A_1$ gives

$$D_1(\bar{S}) = a_{11}m_{22} + a_{21}a_{12} = -m_{22}\psi(\bar{S}) + \left[f'(\bar{S})\bar{u} + g'(\bar{S})\bar{v}\right]m_{22} + f'(\bar{S})\bar{u}a_{12} - ba_{12}.$$

Since

$$m_{22}\psi(\bar{S}) + ba_{12} = \varphi(\bar{S})\left(\psi(\bar{S}) - b\right) = a\bar{u}\psi(\bar{S}), \tag{A.3}$$

it follows that

$$D_1(\bar{S}) = f'(\bar{S})\bar{u}(a_{12} + m_{22}) + g'(\bar{S})\bar{v}m_{22} - a\bar{u}\psi(\bar{S}). \tag{A.4}$$

Replacing u by its expression (8), m_{22} can be rewritten as

$$m_{22} = -b\frac{\varphi(\bar{S})}{\psi(\bar{S})} + a\bar{u} + b \tag{A.5}$$

which is positive. Therefore,

$$m_{22} = \frac{-\varphi\psi + 2\varphi(\psi - b) + b\psi}{\psi} \quad \text{and} \quad a_{12} + m_{22} = -\frac{(\psi - b)(\psi - 2\varphi)}{\psi}.$$

According to (7), we can replace φ/ψ by $-v/u$ in the function $H'(\cdot)$ given by (11) and so we obtain

$$H' = -f'\frac{a_{12} + m_{22}}{a\psi} - g'v\frac{m_{22}}{au\psi}.$$

Multiplying $(H' + 1)$ by $au\psi$ finally yields the following expression

$$D_1(\bar{S}) = -a\bar{u}\psi(\bar{S})\left[1 + H'(\bar{S})\right]. \tag{A.6}$$

From the expression (A.5) of m_{22} and the equations (7-8), a straightforward calculation of $T_1(\bar{S}) := \operatorname{tr} A_1$ gives

$$T_1(\bar{S}) = -\left[f'(\bar{S})\bar{u} + g'(\bar{S})\bar{v} + a\bar{u} + a\frac{\bar{u}^2}{\bar{v}} + b\frac{\bar{v}}{\bar{u}}\right].$$

In the case $\bar{S} \in I$, we have $a_{12} > 0$ and $\psi(\bar{S}) < 0$. From expression (A.6), $D_1(\bar{S}) > 0$ if and only if $H'(\bar{S}) > -1$. From (A.4), it follows that

$$D_1(\bar{S}) > 0 \quad \Longleftrightarrow \quad -a\bar{u}\psi(\bar{S}) + g'(\bar{S})\bar{v}m_{22} > -f'(\bar{S})\bar{u}(a_{12} + m_{22}). \tag{A.7}$$

Dividing this last inequality by $a_{12} + m_{22}$, we obtain

$$-f'(\bar{S})\bar{u} < -\frac{a\bar{u}}{a_{12} + m_{22}}\psi(\bar{S}) + g'(\bar{S})\bar{v}\frac{m_{22}}{a_{12} + m_{22}} < -\psi(\bar{S}) + g'(\bar{S})\bar{v}$$

since $a_{12} + m_{22} = a\bar{u} + P$ with P and $-\psi(\bar{S})$ are positive. Thus $a_{11} > 0$ and so one has $T_1(\bar{S}) = -(a_{11} + m_{22}) < 0$. Consequently, if $H'(\bar{S}) > -1$, then E_1 is LES. Finally, if $H'(\bar{S}) < -1$, then $D_1(\bar{S}) < 0$ and we deduce that E_1 is unstable.

In case $\bar{S} \in J_b$, we have $\psi(\bar{S}) > 0$. From expression (A.6), if $H'(\bar{S}) > -1$, it follows that $D_1(\bar{S}) < 0$ and so E_1 is unstable. This completes the proof. ■

Proof of Prop. 4.1. The equilibria of (2) are solutions of the following system of equations

$$\begin{cases} D(S_{in} - S) &= f(S)u + g(S)v - f_2(S)x_2 \\ 0 &= f(S)u - au^2 + bv - Du \\ 0 &= g(S)v + au^2 - bv - Dv \\ 0 &= [f_2(S) - D]\, x_2. \end{cases} \tag{A.8}$$

The fourth equation gives $x_2 = 0$ or $S = \lambda_2$. If $x_2 = 0$ then, according to Prop. 3.1, we deduce the existence of equilibria F_0 and F_1. If $x_2 \neq 0$ and $u = 0$, then one has $S = \lambda_2$, $v = 0$ and the first equation leads to the equality $x_2 = S_{in} - \lambda_2$. Thus, the equilibrium $F_2 = (\lambda_2, 0, 0, S_{in} - \lambda_2)$ exists if and only if $\lambda_2 < S_{in}$. If $x_2 \neq 0$ and $u \neq 0$, then $S = \lambda_2$, $v \neq 0$ and from the proof of Prop. 3.1, it follows that $u = U(\lambda_2)$ and $v = V(\lambda_2)$ which are positive if and only if $\lambda_2 \in I \cup J_b$. From the first equation of (A.8), we obtain $x_2 = S_{in} - \lambda_2 - H(\lambda_2)$ which is positive if and only if $S_{in} - \lambda_2 > H(\lambda_2)$. ■

For convenience, we denote $\varphi_2(S) = f_2(S) - D$ for the second species. Let J be the Jacobian matrix of (14) at (S, u, x_2), that we write with the following notation

$$J = \begin{bmatrix} -a_{11} & -a_{12} & -a_{13} \\ a_{21} & -m_{22} & -b \\ m_{31} & 0 & a_{33} \end{bmatrix} \tag{A.9}$$

where

$$a_{11} = -\psi(S) + f'(S)u + g'(S)(S_{in} - S - u - x_2) + f_2'(S)x_2, \quad a_{12} = f(S) - g(S), \quad a_{13} = f_2(S) - g(S),$$

$$a_{21} = f'(S)u - b, \quad m_{22} = -\varphi(S) + 2au + b, \quad m_{31} = f_2'(S)x_2 \quad \text{and} \quad a_{33} = \varphi_2(S).$$

Proof of Prop. 4.2.

1. At the washout equilibrium $F_0 = (S_{in}, 0, 0, 0)$, we have $Z = S_{in}$. Thus, it suffices to prove that $\mathbb{F}_0 = (S_{in}, 0, 0)$ is a LES equilibrium of the reduced system (14). From (A.9), the Jacobian matrix of (14) at $\mathbb{F}_0$ is given by

$$J_0 = \begin{bmatrix} & & g(S_{in}) - f_2(S_{in}) \\ & A_0 & -b \\ 0 & 0 & \varphi_2(S_{in}) \end{bmatrix}$$

where A_0 is the 2×2 Jacobian matrix (12) at $\mathbb{E}_0$. The eigenvalues of J_0 are the eigenvalues of A_0 and $\varphi_2(S_{in})$. From Prop. 3.4, one can conclude that the equilibrium F_0 is LES if and only if $\varphi(S_{in}) < 0$ and $S_{in} < \min(\lambda_b, \lambda_2)$.

2. At the equilibrium $F_2 = (\lambda_2, 0, 0, \bar{x}_2)$ where $\bar{x}_2 = S_{in} - \lambda_2$, we have $Z = S_{in}$. It suffices to prove that $\mathbb{F}_2 = (\lambda_2, 0, \bar{x}_2)$ is a LES equilibrium of the reduced system (14). From (A.9), the Jacobian matrix of (14) at $\mathbb{F}_2$, is given by

$$J_2 = \begin{bmatrix} \psi(\lambda_2) - f_2'(\lambda_2)\bar{x}_2 & \psi(\lambda_2) - \varphi(\lambda_2) & \psi(\lambda_2) \\ -b & \varphi(\lambda_2) - b & -b \\ f_2'(\lambda_2)\bar{x}_2 & 0 & 0 \end{bmatrix}.$$

The characteristic polynomial is given by $P(\lambda) = \det(J_2 - \lambda I)$, where I is the 3×3 identity matrix.
Denote C_i and L_i the columns and lines of the matrix $J_2 - \lambda I$. The replacements of C_1 by $C_1 - C_3$ and L_3 by $L_3 + L_1$ preserve the determinant and one has

$$P(\lambda) = \begin{vmatrix} -f_2'(\lambda_2)\bar{x}_2 - \lambda & \psi(\lambda_2) - \varphi(\lambda_2) & \psi(\lambda_2) \\ 0 & \varphi(\lambda_2) - b - \lambda & -b \\ 0 & \psi(\lambda_2) - \varphi(\lambda_2) & \psi(\lambda_2) - \lambda \end{vmatrix}.$$

Moreover, the replacements of C_1 by $C_1 - C_2$ and L_2 by $L_1 + L_2$ lead to

$$P(\lambda) = (-f_2'(\lambda_2)\bar{x}_2 - \lambda) \begin{vmatrix} \varphi(\lambda_2) - \lambda & -b \\ 0 & \psi(\lambda_2) - b - \lambda \end{vmatrix}.$$

Therefore,

$$-f_2'(\lambda_2)\bar{x}_2, \quad \varphi(\lambda_2) \quad \text{and} \quad \psi(\lambda_2) - b$$

are the eigenvalues of J_2. We conclude that F_2 is LES if and only if $\varphi(\lambda_2) < 0$ and $\lambda_2 < \lambda_b$.

3. At the equilibrium $F_1 = (\bar{S}, \bar{u}, \bar{v}, 0)$, it is easy to see from Prop. 4.1 that $Z = \bar{S} + \bar{u} + \bar{v} = S_{in}$. Then, it suffices to prove that $\mathbb{F}_1 = (\bar{S}, \bar{u}, 0)$ is a LES equilibrium of the reduced system (14). From (A.9), the Jacobian matrix of (14) at $\mathbb{F}_1$, is given by

$$J_1 = \begin{bmatrix} & & g(\bar{S}) - f_2(\bar{S}) \\ & A_1 & -b \\ 0 & 0 & \varphi_2(\bar{S}) \end{bmatrix}.$$

The eigenvalues of this matrix are the eigenvalues of the 2×2 sub-matrix A_1 and $\varphi_2(\bar{S})$. From Prop. 3.5, it follows that F_1 is LES if and only if $\bar{S} < \lambda_2$ and the condition (13) holds.

■

Proof of Prop. 4.3. We denote with a * the quantities evaluating at the positive equilibrium $F^* = (\lambda_2, u^*, v^*, x_2^*)$.

It is easy to see from Prop. 4.1 that $Z^* = \lambda_2 + u^* + v^* + x_2^* = S_{in}$. Then, it suffices to prove that $\mathbb{F}^* = (\lambda_2, u^*, x_2^*)$ is a LES equilibrium of the reduced system (14). Let J^* denote the Jacobian matrix of reduced system (14) at the equilibrium $\mathbb{F}^*$. The characteristic polynomial is given by $P(\lambda) = \det(J^* - \lambda I) = c_0\lambda^3 + c_1\lambda^2 + c_2\lambda + c_3$, where

$$c_0 = -1, \quad c_1 = -(a_{11} + m_{22}), \quad c_2 = -(m_{22}a_{11} + a_{21}a_{12} + a_{13}m_{31}) \quad \text{and} \quad c_3 = m_{31}(ba_{12} - m_{22}a_{13}).$$

According to Routh-Hurwitz criterion, $\mathbb{F}^*$ is LES if and only if

$$\begin{cases} c_i < 0, & i = 0, \ldots, 3 \\ c_1c_2 - c_0c_3 > 0. \end{cases} \tag{A.10}$$

From equation (A.3), we obtain

$$c_3 = m_{31}au^*\psi(\lambda_2)$$

If $\lambda_2 \in J_b$, then $c_3 > 0$ and so the Routh-Hurwitz criterion implies that $\mathbb{F}^*$ is unstable. In the following, we consider the case $\lambda_2 \in I$ and $H'(\lambda_2) > -1$. From (A.6) and (A.7), we deduce that

$$-au^*\psi(\lambda_2) + f'(\lambda_2)u^*(a_{12} + m_{22}) + g'(\lambda_2)v^*m_{22} > 0\,. \tag{A.11}$$

From (A.3), we obtain

$$m_{22}a_{11} + a_{21}a_{12} = m_{22}\left[f'(\lambda_2)u^* + g'(\lambda_2)v^* + m_{31}\right] - au^*\psi(\lambda_2) + a_{12}f'(\lambda_2)u^*$$

which is positive from (A.11). Consequently one has $c_2 < 0$ because $a_{13}m_{31}$ is positive. Since $a_{12} > 0$ in this case, one can divide inequality (A.11) by $a_{12} + m_{22}$ and obtain

$$-f'(\lambda_2)u^* < -\frac{au^*}{a_{12} + m_{22}}\psi(\lambda_2) + g'(\lambda_2)v^*\frac{m_{22}}{a_{12} + m_{22}} < -\psi(\lambda_2) + g'(\lambda_2)v^*$$

because $a_{12} + m_{22} = au^* + P$ with P and $-\psi(\lambda_2)$ are positive. Thus, $a_{11} > 0$ and so $c_1 < 0$. Then, a straightforward calculation gives

$$c_1c_2 - c_0c_3 = (a_{11} + m_{22})(m_{22}a_{11} + a_{21}a_{12}) + a_{11}a_{13}m_{31} + ba_{12}m_{31}$$

which is positive. Therefore all the conditions of the Routh-Hurwitz criterion are satisfied and thus F^* is LES. ■

Appendix B. Parameters used in numerical simulations

All the values of the parameters values, for the one and two species models, respectively, are given in Tables B.4 and B.5.

Parameter	m_{11}	K_{11}	K_i	m_{12}	K_{12}	D	a	b	S_{in}	λ_0	μ_0	λ_1	λ_b
Fig. 2(a)	2.7	1	1.2	1.5	1	0.9	0.1	0.27	3	0.710	1.690	1.5	3.545
Fig. 2(c)	3	0.1	0.01	1	2	0.1	2	2	15	0.003	0.286	0.222	$+\infty$
Fig. 3(a)	2.7	0.5	1.2	1.3	1	0.9	0.1	0.15	Variable	0.283	2.117	2.25	4.2
Figs. 4(a-b)									Variable				
Fig. 5	3	1	1.2	1.5	1	0.9	0.005	0.3	9.8	0.528	2.272	1.5	4
Fig. 4(c)									9.95				

Table B.4: Parameter values and corresponding values λ_0, μ_0, λ_1 and λ_b.

Parameter	m_{11}	K_{11}	K_i	m_{12}	K_{12}	D	a	b	S_{in}	m_2	K_2
Fig. 6(a)	2.7	1	1.2	1.5	1	0.9	0.1	0.27	3	3	2
Fig. 6(b)										1.8	
Figs. 7, 8 and 9	3	0.5	1.2	1.25	1.5	0.9	2	2	3.5	Variable	2
Figs. 10, 11, 12 and 13									3.65		

Table B.5: Parameter values for the two species model.

Acknowledgments

The authors wish to thank the financial support of TREASURE euro-Mediterranean research network (https://project.inria.fr/treasure/). This work has been achieved during the preparation of the PhD of the first author within the INRA/INRIA team MODEMIC, with the financial support of the Averroes program, the PHC UTIQUE project No. 13G1120 and the COADVISE project.

References

[1] G.J. Butler and G.S.K. Wolkowicz. A mathematical model of the chemostat with a general class of functions describing nutrient uptake. *SIAM J. Appl. Math.*, 45, (1):138–151, 1985.

[2] R. Fekih-Salem, J. Harmand, C. Lobry, A. Rapaport, and T. Sari. Extensions of the chemostat model with flocculation. *J. Math. Anal. Appl.*, 397, (1):292–306, 2013.

[3] R. Fekih-Salem, T. Sari, and N. Abdellatif. Sur un modèle de compétition et de coexistence dans le chemostat. *ARIMA J.*, 14:15–30, 2011.

[4] R. Fekih-Salem, T. Sari, and A. Rapaport. La floculation et la coexistence dans le chemostat. In *Proceedings of the 5th conference on Trends in Applied Mathematics in Tunisia, Algeria, Morocco*, pages 477–483, 2011.
[5] R. Freter, H. Brickner, and S. Temme. An understanding of colonization resistance of the mammalian large intestine requires mathematical analysis. *Microecology and Therapy*, 16:147–155, 1986.
[6] J.P. Grover. *Resource Competition*. Chapman and Hall, London, 1997.
[7] B. Haegeman, C. Lobry, and J. Harmand. Modeling bacteria flocculation as density-dependent growth. *AIChE J.*, 53, (2):535–539, 2007.
[8] B. Haegeman and A. Rapaport. How flocculation can explain coexistence in the chemostat. *J. Biol. Dyn.*, 2, (1):1–13, 2008.
[9] S.R. Hansen and S.P. Hubbell. Single-nutrient microbial competition: qualitative agreement between experimental and theoretically forecast outcomes. *Science*, 207, (4438):1491–1493, 1980.
[10] G. Hardin. The competitive exclusion principale. *Science*, 131, (3409):1292–1297, 1960.
[11] J. Heßeler, J.K. Schmidt, U. Reichl, and D. Flockerzi. Coexistence in the chemostat as a result of metabolic by-products. *J. Math. Biol*, 53, (4):556–584, 2006.
[12] S.B. Hsu. Limiting behavior for competing species. *SIAM J. Appl. Math.*, 34, (4):760–763, 1978.
[13] G.E. Hutchinson. The paradox of the plankton. *Am. Nat.*, 95, (882):137–145, 1961.
[14] D. Jones, H.V. Kojouharov, D. Le, and H.L. Smith. The Freter model: A simple model of biofilm formation. *J. Math. Biol.*, 47:137–152, 2003.
[15] Yu.A. Kuznetsov. *Elements of Applied Bifurcation Theory*. Third edition. Springer, New York, 2004.
[16] P. De Leenheer, D. Angeli, and E.D. Sontag. Crowding effects promote coexistence in the chemostat. *J. Math. Anal. Appl.*, 319:48–60, 2006.
[17] Z. Li, L. Chen, and Z. Liu. Periodic solution of a chemostat model with variable yield and impulsive state feedback control. *Applied Mathematical Modelling*, 36, (3):1255–1266, 2012.
[18] C. Lobry and J. Harmand. A new hypothesis to explain the coexistence of n species in the presence of a single resource. *C. R. Biologies*, 329:40–46, 2006.
[19] C. Lobry, A. Rapaport, and F. Mazenc. Sur un modèle densité-dépendant de compétition pour une ressource. *C. R. Biologies*, 329:63–70, 2006.
[20] P.R. Patnaik. Dynamic sensitivity of a chemostat for a microbial reaction with substrate and product inhibition. *Applied Mathematical Modelling*, 18, (11):620–627, 1994.
[21] S. Pilyugin and P. Waltman. The simple chemostat with wall growth. *SIAM J. Appl. Math.*, 59, (5):1552–1572, 1999.
[22] T. Sari. A Lyapunov function for the chemostat with variable yields. *C. R. Acad. Sci. Paris, Ser. I*, 348:747–751, 2010.
[23] T. Sari. Competitive exclusion for chemostat equations with variable yields. *Acta Appl. Math.*, 123, (1):201–219, 2013.
[24] T. Sari and F. Mazenc. Global dynamics of the chemostat with different removal rates and variable yields. *Math. Biosci. Eng.*, 8, (3):827–840, 2011.
[25] M. Scheffer, S. Rinaldi, J. Huisman, and F.J. Weissing. Why plankton communities have no equilibrium: solutions to the paradox. *Hydrobiologia*, 491:9–18, 2003.
[26] J.K. Schmidt, B. König, and U. Reichl. Characterization of a three bacteria mixed culture in a chemostat: Evaluation and application of a quantitative Terminal-Restriction Fragment Length Polymorphism (T-RFLP) analysis for absolute and species specific cell enumeration. *Biotechnol. Bioeng.*, 96, (4):738–756, 2007.
[27] H.L. Smith and P. Waltman. *The Theory of the Chemostat : Dynamics of Microbial Competition*. Cambridge University Press, 1995.
[28] B. Tang, A. Sitomer, and T. Jackson. Population dynamics and competition in chemostat models with adaptive nutrient uptake. *J. Math. Biol.*, 35:453–479, 1997.
[29] G.S.K. Wolkowicz and Z. Lu. Global dynamics of a mathematical model of competition in the chemostat: General response functions and differential death rates. *SIAM J. Appl. Math.*, 52:222–233, 1992.
[30] G.S.K. Wolkowicz and Z. Lu. Direct interference on competition in a chemostat. *J. Biomath*, 13, (3):282–291, 1998.
[31] L.Y. Zhang. Hopf bifurcation analysis in a Monod-Haldane predator-prey model with delays and diffusion. *Applied Mathematical Modelling*, 39, (3-4):1369–1382, 2015.
[32] X. Zhou, X. Song, and X. Shi. Analysis of competitive chemostat models with the Beddington-DeAngelis functional response and impulsive effect. *Applied Mathematical Modelling*, 31, (10):2299–2312, 2007.